

## Epitaxial diamond encapsulation of metal microprobes for high pressure experiments

Samuel T. Weir,<sup>a)</sup> Jagannadham Akella, and Chantel Aracne-Ruddle  
Lawrence Livermore National Laboratory, University of California, Livermore, California 94550

Yogesh K. Vohra and Shane A. Catledge  
Department of Physics, University of Alabama at Birmingham, Birmingham, Alabama 35294

(Received 17 April 2000; accepted for publication 19 September 2000)

Diamond anvils with diamond encapsulated thin-film microcircuits have been fabricated for ultrahigh pressure electrical conductivity experiments. The diamond films were homoepitaxially deposited onto the diamond anvil substrates with microwave plasma chemical vapor deposition using a 2% methane in hydrogen gas mixture and a diamond substrate temperature of 1300 °C. The diamond embedded thin-film microprobes remain functional to megabar pressures. We have applied this technology to the study of the pressure-induced metallization of KI under pressures up to 1.8 Mbar. This technology has the potential of greatly advancing the pressure range of a number of existing high-pressure diagnostic techniques, and for expanding the capabilities of diamond anvil cells into new directions. © 2000 American Institute of Physics. [S0003-6951(00)00347-8]

Ultrahigh pressure experiments utilizing diamond anvil cells (DACs) have been instrumental in revealing new and unexpected high-pressure phases and new physical phenomena under extreme compressions. A wide range of diagnostic probes have been utilized for studying the physical and structural properties of materials under ultrahigh static pressures, including x-ray diffraction,<sup>1</sup> Raman spectroscopy,<sup>1</sup> optical absorption,<sup>1</sup> electrical conductivity,<sup>1,2</sup> magnetic susceptibility,<sup>3,4</sup> and nuclear magnetic resonance.<sup>5</sup> Recently, electrical conductivity experiments have been performed to megabar pressures using diamond anvil cells with alumina insulating gaskets and thin foil platinum electrodes.<sup>6–8</sup> However, continuing experimental difficulties related to the very small size of a DAC sample and its physical inaccessibility still limit the full utilization of many valuable diagnostic probes, including electrical conductivity, magnetic susceptibility, and nuclear magnetic resonance (NMR), to pressures significantly below the maximum attainable DAC pressure of approximately 5 million atm (5 Mbar or 500 GPa). Here, we report on the development of a technology for fabricating diamond encapsulated thin-film metal microcircuits on a diamond anvil substrate. These circuits remain functional under multimegabar pressures, and overcome many diagnostic difficulties related to small DAC sample sizes and high shearing stresses around the sample. We have applied this technology to the study of the pressure-induced metallization of KI under pressures up to 1.8 Mbar. We anticipate that this technology will have a significant impact on advancing the capabilities of a number of static high-pressure techniques which would benefit from the ability to place customizable, diamond-embedded microcircuits in immediate proximity to an ultrahigh pressure sample.

While microlithographic fabrication of thin-film metal circuits directly onto diamond anvils has been performed

previously by other experimenters,<sup>9,10</sup> the encapsulation of such circuits in a layer of high-quality, synthetic diamond is a development which greatly enhances their survivability. High-pressure experiments have shown that the shearing stresses present in a DAC at megabar pressures can exceed 10 GPa,<sup>11</sup> which can result in considerable plastic flow and damage of unprotected thin film circuits. Thus, diamond encapsulation is crucial for ensuring circuit survivability at multimegabar pressures. Diamond is ideally suited for this purpose because of its extremely high compressive strength and very large shear modulus. Additionally, diamond has been predicted to remain an electrical insulator to pressures far in excess of 5 Mbar.<sup>12,13</sup> Our work has been enabled by recent technological advances in homoepitaxial diamond deposition with high growth rates.<sup>14</sup> By depositing the diamond film homoepitaxially onto the diamond anvil substrate, an extremely strong diamond film-to-anvil bond is created, with an adhesion strength approaching that of single-crystal diamond. Figure 1 shows a simplified schematic diagram of a designer anvil as it would be used in a diamond anvil cell.

For the starting substrate, we typically utilize a 1/3 carat (67 mg) type-Ia diamond anvil with a polished culet oriented

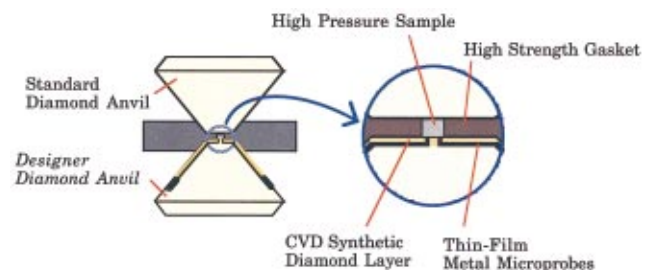


FIG. 1. (Color) Simplified schematic diagram of a designer anvil. Ultrahigh sample pressures are generated by forcing the two anvils together. The magnified view shows the high-pressure region between the two anvils. The designer anvil features a set of thin-film metal microprobes and a protective chemical vapor deposited diamond layer (shown in orange) encasing the microprobes.

<sup>a)</sup>Author to whom correspondence should be addressed; electronic mail: weir3@llnl.gov

in the (100) plane. A set of four thin-film metal microprobes is then fabricated onto the anvil. This is accomplished by first depositing a 2  $\mu\text{m}$  layer of polymethyl methacrylate photoresist onto the anvil, and then exposing the desired mask pattern consisting of four 10  $\mu\text{m}$  wide probes with the mercury ultraviolet *g* and *h* lines ( $\lambda=436\text{ nm}$  and  $\lambda=405\text{ nm}$ ) of a lithographic projection aligner. After photoresist exposure and development, the photoresist pattern is extended down the sides of the anvil, and a 7000  $\text{\AA}$  layer of tungsten is sputter deposited onto the anvil. Tungsten is an attractive choice for the microprobes for several reasons. First, as a carbide-forming metal, tungsten forms a very strong bond to the diamond anvil substrate. Second, since tungsten is a refractory metal ( $T_{\text{melt}}=3410\text{ }^\circ\text{C}$ ), it is capable of surviving the high substrate temperatures required for epitaxial diamond deposition ( $\approx 1300\text{ }^\circ\text{C}$ ) without melting or diffusing into the surrounding diamond. Tungsten also has a relatively low coefficient of thermal expansion [ $\alpha_{\text{W}}=4.5 \times 10^{-6}\text{ }^\circ\text{C}^{-1}$ @room temperature (RT)], and so thermally induced stresses between the tungsten film and the diamond substrate ( $\alpha_{\text{DIA}}=1.5 \times 10^{-6}\text{ }^\circ\text{C}^{-1}$ @RT) are minimized. Finally, interfacial stresses induced by mismatched elastic constants under high pressures are minimized because, like diamond, tungsten has an extremely high bulk modulus ( $B=308\text{ GPa}$  versus diamond's  $B=442\text{ GPa}$ ) and has no pressure-induced structural phase transition to at least 4 Mbar.<sup>15,16</sup>

After fabrication of the tungsten microprobes, a layer of high-quality, epitaxial diamond was deposited onto the anvil substrate by microwave plasma chemical vapor deposition using a 2% methane in hydrogen gas mixture.<sup>17</sup> The microwave magnetron source operates at a frequency of 2.45 GHz and a power of about 1000–1100 W. Previous experiments have shown that this system is capable of growing homoepitaxial diamond onto a diamond anvil substrate at a substrate temperature of approximately 1300  $^\circ\text{C}$  and a chamber pressure of 90 Torr. Typical diamond film growth rates are about 15  $\mu\text{m}/\text{h}$ , and the final film thickness is normally 40–70  $\mu\text{m}$ .

The direct deposition of diamond onto metals is difficult, and metal substrates are usually seeded with diamond powder or abraded ultrasonically to facilitate diamond nucleation. For an unseeded tungsten surface, a long incubation time is required in order to first carburize the surface of the tungsten film, and then subsequently nucleate diamond onto the tungsten carbide phase. In our case, the tungsten microprobes were not seeded, and so the incubation times for diamond nucleation are expected to be large (several hours). Therefore, homoepitaxial diamond growth onto the surrounding diamond substrate appears to be the predominant growth mechanism. The success of our microprobe encapsulation technique is based on the high growth rate of the homoepitaxial diamond film, which bridges over and completely encases the tungsten microprobes. The high quality of the diamond film, evident from its high transparency, was confirmed by photoluminescence and micro-Raman spectroscopy which revealed that the film consists largely of  $sp^3$ -bonded diamond, although small amounts of  $sp^2$ -bonded carbon are also present, particularly in the vicinity of the microprobes.

To prepare the diamond anvil for a high-pressure experiment, the diamond film was polished to a smooth finish and

Emerging microprobe

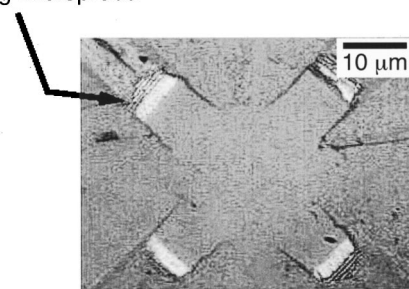


FIG. 2. A high-magnification picture of a completed designer anvil. This picture of the center of a designer diamond anvil culet shows the metal microprobes emerging from beneath the synthetic diamond layer in order to make electrical contact with the sample.

shallow 7.5° bevels were added. The thickness of the diamond film after polishing is typically 10–20  $\mu\text{m}$ . Figure 2 shows the central flat region of a completed anvil, illustrating how the metal microprobes emerge from beneath the synthetic diamond film in order to make electrical contact with the sample.

The ultrahigh pressure performance of our designer anvil was demonstrated by an electrical conductivity experiment on the compound KI. KI is an ionic solid crystallizing in the rock-salt (B1) structure, and is optically transparent at ambient pressure with an electronic band gap of 6.0 eV. Under high pressures, KI undergoes a structural phase transition to the cesium–chloride (B2) structure at 1.9 GPa.<sup>18</sup> By extrapolating optical absorption experiments examining the band-edge threshold energy to pressures of 70 GPa, it was predicted that KI would metallize by means of an indirect band overlap transition at a pressure of approximately 115 GPa.<sup>18</sup>

In our experiment we used a designer anvil together with a matching standard anvil. The culets of both anvils were approximately 300  $\mu\text{m}$  in diameter, and their central flats were both about 70  $\mu\text{m}$  in diameter. A bevel angle of 7.5° was used for both the designer anvil and the matching anvil. An alumina gasket was used, and a KI sample was placed in a sample chamber of about 70  $\mu\text{m}$  in diameter located at the center of the culet. The sample pressure was determined by means of energy-dispersive x-ray diffraction of the KI sample itself, using the isothermal,  $P$ – $V$  equation-of-state (EOS) of Asaumi *et al.*<sup>18</sup> Their EOS data were taken up to pressures of 70 GPa, so sample pressures above this were based on an extrapolation of their Birch–Murnaghan EOS parameters.

Figure 3 shows a plot of pressure versus KI sample resistance obtained with the designer anvil experiment. Resistance was measured using a dc two-probe technique with a current of 100  $\mu\text{A}$ . The resistance of the microprobes themselves was 110  $\Omega$ , and so this value was subtracted from the total probe-to-probe resistance to obtain the sample resistance. For pressures below 90 GPa, the resistance was unmeasurably large, but above this pressure the resistance was observed to drop rapidly with increasing pressure, as expected for conduction by thermally activated charge carriers across a decreasing band gap. With further increases in pressure, the resistance eventually saturates to an approximately constant value for pressures above 140 GPa. From the pressure dependence of the resistance and the intersection of the

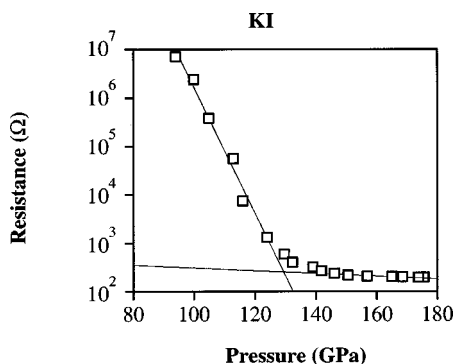


FIG. 3. KI resistance vs pressure. Below approximately 130 GPa the resistance drops rapidly with increasing pressure in a manner consistent with semiconducting behavior. Above 140 GPa, the resistance levels out to an approximately constant value, which we interpret as metallization. We identify the metallization pressure as 131 GPa based on the intersection of the two line fits (shown as solid lines) of the characteristic resistance vs pressure behavior at low (<120 GPa) and high (>140 GPa) pressures.

two least-squares line fits of the characteristic resistance versus pressure behavior at low and high pressures (<120 GPa and >140 GPa), we identify the metallization pressure of KI as being approximately 131 GPa. For comparison, electronic band-structure calculations by Amirthakumari *et al.*<sup>19</sup> predicted band-overlap metallization at 126 GPa; the Herzfeld criterion<sup>20</sup> predicts metallization at 98 GPa, and the band edge absorption experiments by Asaumi *et al.*<sup>18</sup> predicted metallization by indirect band overlap at 115 GPa.

The advent of megabar-survivable, diamond encapsulated microcircuits offers exciting possibilities for greatly increasing the pressure range of many *in situ* static high-pressure diagnostic techniques such as electrical conductivity, magnetization, and NMR, and for expanding the capabilities of diamond anvil cells in new directions. Thus, we expect that this technology will lead to the discov-

ery of much more science on materials subjected to extreme pressures in diamond anvil cells.

The authors thank Dino Ciarlo and Ron Lee for helpful discussions, and Steve Falabella Vince Malba, Kouros Ghandehari, and Jingzhu Hu for technical help, and L. T. Wiley and B. T. Goodwin for support of this work. This work was performed under the auspices of the U.S. Department of Energy by the University of California, Lawrence Livermore National Laboratory under Contract No. W-7405-Eng-48.

- <sup>1</sup>A. Jayaraman, *Rev. Mod. Phys.* **55**, 65 (1983).
- <sup>2</sup>S. T. Weir and A. L. Ruoff, *Scr. Metall.* **22**, 151 (1988).
- <sup>3</sup>M. Ishizuka, K. Amaya, and S. Endo, *Rev. Sci. Instrum.* **66**, 3307 (1995).
- <sup>4</sup>V. Struzhkin, R. J. Hemley, H-K. Mao, and Y. A. Timofeev, *Nature (London)* **390**, 382 (1997).
- <sup>5</sup>M. G. Pravica and I. F. Silvera, *Rev. Mod. Instrum.* **69**, 479 (1998).
- <sup>6</sup>M. I. Eremets, K. Shimizu, T. C. Kobayashii, and K. Amaya, *Science* **281**, 1333 (1998).
- <sup>7</sup>K. Shimizu, K. Suhara, M. Ikumo, M. I. Eremets, and K. Amaya, *Nature (London)* **393**, 767 (1998).
- <sup>8</sup>K. Amaya, K. Shimizu, M. I. Eremets, T. C. Kobayashi, and S. Endo, *J. Phys.: Condens. Matter* **10**, 11179 (1998).
- <sup>9</sup>T. A. Grzybowski and A. L. Ruoff, *Phys. Rev. Lett.* **53**, 489 (1984).
- <sup>10</sup>H. Hemmes, A. Driessen, J. Kos, F. A. Mul, R. Griessen, J. Caro, and S. Radelaar, *Rev. Sci. Instrum.* **60**, 474 (1989).
- <sup>11</sup>R. J. Hemley, H-K. Mao, G. Shen, J. Badro, P. Gillet, M. Hanfland, and D. Hauserman, *Science* **276**, 1242 (1997).
- <sup>12</sup>A. L. Ruoff, H. Luo, and Y. K. Vohra, *J. Appl. Phys.* **69**, 6413 (1991).
- <sup>13</sup>A. L. Ruoff and H. Luo, *J. Appl. Phys.* **70**, 2066 (1991).
- <sup>14</sup>K. A. Snail and L. M. Hanssen, *J. Cryst. Growth* **112**, 651 (1991).
- <sup>15</sup>A. L. Ruoff, H. Xia, H. Luo, and Y. K. Vohra, *Rev. Sci. Instrum.* **61**, 3830 (1990).
- <sup>16</sup>A. L. Ruoff, J. Xia, and Q. Xia, *Rev. Sci. Instrum.* **63**, 4342 (1992).
- <sup>17</sup>S. A. Catledge, Y. K. Vohra, S. T. Weir, and J. Akella, *J. Phys.: Condens. Matter* **9**, 67 (1997).
- <sup>18</sup>K. Asaumi, T. Suzuki, and T. Mori, *Phys. Rev. B* **28**, 3529 (1983).
- <sup>19</sup>R. M. Amirthakumari, G. Pari, R. Rita, and R. Asokamani, *Phys. Status Solidi B* **199**, 157 (1997).
- <sup>20</sup>K. F. Herzfeld, *Phys. Rev.* **29**, 701 (1927).